

CrossMark
click for updatesCite this: *RSC Adv.*, 2014, 4, 63118

Macromolecular chain structure design, synthesis and analysis of poly(L-lactide) linking ultraviolet absorbing groups

Feijie Ge, Yun Huang, Yu Luo, Long Jiang* and Yi Dan*

Poly(L-lactide) (PLA) with different chain structures was designed, and successfully synthesized by ring opening polymerization using 2-hydroxy-4-(3-methacryloxy-2-hydroxypropoxy) benzophenone (BPMA), 2,2'-dihydroxy-4,4'-(2-hydroxypropoxy) dibenzophenone (DHDBP) and 2-hydroxy-4-(2,3-dihydroxypropoxy) benzophenone (HPBP) as initiators, respectively, to produce corresponding PLA-B (end-capped with BPMA), PLA-DB (end-capped with DHDBP) and PLA-HB-PLA (blocked with HPBP in the middle). High-molecular-weight PLA-DB400 with good visible light transparency and UV opacity was prepared. The chemical structures of the samples were characterized, the crystallization behavior, thermal stability, UV absorption properties and transmittance of PLA were investigated and analyzed. Results of GPC and DSC reveal that when the number average molecular weights (M_n) of PLA are around 4000, termination of a UV absorbing group like DHDBP greatly restricts the crystallization of PLA due to the larger volume and rigidity of the end-capping group, but increasing M_n to about 12 000 or higher weakens the hindering effect, resulting in a similar degree of crystallization (X_c). TG results show that PLA-DB400 has the best thermal stability due to the highest molar mass. When the UV absorber is blocked in the PLA chain, the restriction and steric hindrance of the absorber are much stronger than that in the end-capped material, making X_c significantly reduced. UV absorbance of the PLA solutions reveals that the introduction of UV absorbing groups gives an absorption to UV light below 350 nm and the position of the introduced groups has no influence on the UV absorption properties although the content of the UV group does enhance the UV absorbance, of which PLA-DB has the highest since DHDBP bears two 2-dihydroxybenzophenone groups. The transparency of PLA films is neither affected by position nor content of the introduced UV absorbing groups, which is very beneficial for the application of PLA in packaging materials that require high transparency.

Received 2nd November 2014
Accepted 14th November 2014

DOI: 10.1039/c4ra13631d

www.rsc.org/advances

Introduction

Poly(lactide) (PLA) is a biodegradable aliphatic polyester, and can be synthesized from lactic acid or lactide that originates from renewable resources rich in starch. With good biocompatibility, it has been applied in the biomedical field.^{1,2} As a plastic, PLA has comparable mechanical properties to PS, PP, and can be totally degraded to nontoxic carbon dioxide and water.³ Therefore, with the decreasing cost of PLA and increasing demand for environmental protection, PLA is a promising green polymer material in replacing traditional petroleum-based polymers.⁴ When used as a packaging material, PLA is usually required to have high transparency, UV resistance and relatively good mechanical properties. Since PLA is naturally semicrystalline and brittle,⁴ much attention has been paid to improving its

flexibility.⁵⁻⁸ But compared with many other polymers, PLA has high UV light transmittance⁹ and its degradation is accelerated under UV irradiation, which limits its application in cases requiring UV sterilization and disinfection.^{10,11}

In order to block UV transmission and protect PLA products from UV damage, inorganic particles or nanoparticles including TiO₂, ZnO, nano-Ag, and ZnS with UV resistant property have been used by many researchers to help absorb UV light and improve the UV resistance of PLA. ZnO and anatase TiO₂ accelerate the UV degradation and nano-silver has poor dispersion in PLA matrix.¹²⁻¹⁶ Addition of low molecular weight organic UV absorbers makes better compatibility but worse resistance to organic solvent extraction, and small molecules tend to migrate in PLA products.^{17,18} On the other hand, chemical modifications like synthesis of PLA block copolymers and termination of PLA with rigid large groups, are mainly investigated on their effect on crystallization, hydrolysis or toughening, and little attention were paid to UV absorption or resistant properties.¹⁹⁻²³ Given that macromolecular chain structure essentially affects the physical properties of polymers,

State Key Laboratory of Polymer Materials Engineering of China, Polymer Research Institute, Sichuan University, Chengdu, Sichuan, 610065, P. R. China. E-mail: jianglong@scu.edu.cn; danyichenweiwei@163.com; Fax: +86-28-85402465; Tel: +86-28-85407286

for instance, chain end groups are segregated on the surface of materials, which will change surface properties of polymers,²⁴ and relationship between polymer chain structures of PLA linking UV absorption groups and UV resistance has not been investigated yet, end-capping technique as well as blocking method using different UV absorption groups is herein conducted to introducing UV absorption groups onto PLA chain for investigating the effect of different macromolecular chain structures (with varied positions of introduced UV absorption groups) on the UV absorption property of polylactides, and thereby to figure out the best structure for UV absorption of PLA. Honestly, this consideration makes sense in providing alternative methods for anti-UV chemical modification of polylactides. In this work, PLA with three different chain structures that bear UV absorption groups will be synthesized by ring opening polymerization (ROP) of *L*-lactide using small molecule UV absorbers *via* structure design and analyzed as well. One will be terminated by group from BPMA (producing PLA-B), the second will be terminated by that from DHDBP (resulting in PLA-DB), and the last will be inserted by that from HPBP in the middle of PLA main chain (PLA-HB-PLA). Effect of different polymer chain structures on crystallization, UV absorption and transparency will be investigated.

Experimental

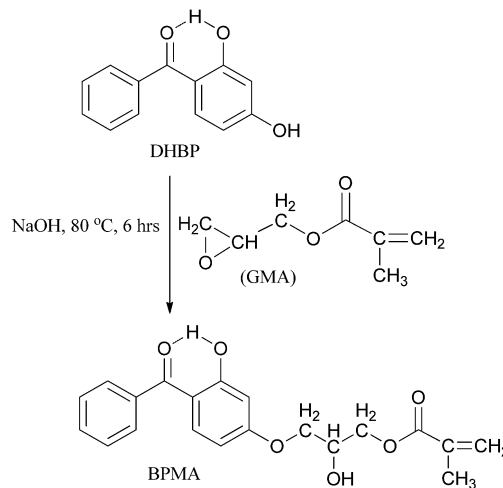
Materials

Glycidyl methacrylate (GMA, 97%), epichlorohydrin (ECH, 99.5%) and 2,4-dihydroxybenzophenone (DHBP, 99%) were provided by Shanghai Jingchun Biochemical Technology Co., Ltd. (Shanghai, China). *L*-Lactide (99.7%, with *D*-lactide content less than 1%) was provided by Shenzhen Brightchina Industrial Co., Ltd. (Shenzhen, China). Tin(II) 2-ethylhexanoate (Sn(Oct)₂, 95%) was purchased from Sigma-Aldrich (Japan). Cetyl alcohol (≥98%), toluene (≥99.5%), chloroform (≥99%), sodium hydroxide (≥96%), ethanol (≥99.7%) and acetone (≥99%) were all of analytical grade and provided by Kelong Chemical Reagent Factory of Chengdu (Chengdu, China). All of the above reactants and reagents were used as received without further purification.

Synthesis of BPMA

The synthesis of BPMA is presented in Scheme 1.

BPMA (2-hydroxy-4-(3-methacryloxy-2-hydroxypropoxy) benzophenone) was synthesized according to literature.²⁵ In brief, DHBP (10.72 g, 50 mmol) was reacted with GMA (7.81 g, 55 mmol) under catalysis of solid NaOH (0.157 g, 3.9 mmol) in a 250 mL three-neck round bottom flask at 80 °C for 6 hours with constant stirring and reflux under nitrogen atmosphere. A yellow viscous liquid was obtained which was then washed with dilute sulfuric acid (0.1 M), extracted by toluene, and finally the excess toluene was evaporated by a rotary evaporator. The crude product was purified through chromatography on silica gel using the mixed solvent of petroleum ether and ethyl acetate (3.5 : 1, v/v) as eluent and dried in vacuum oven at 40 °C for 2 days, and then a yield of 60% was obtained.

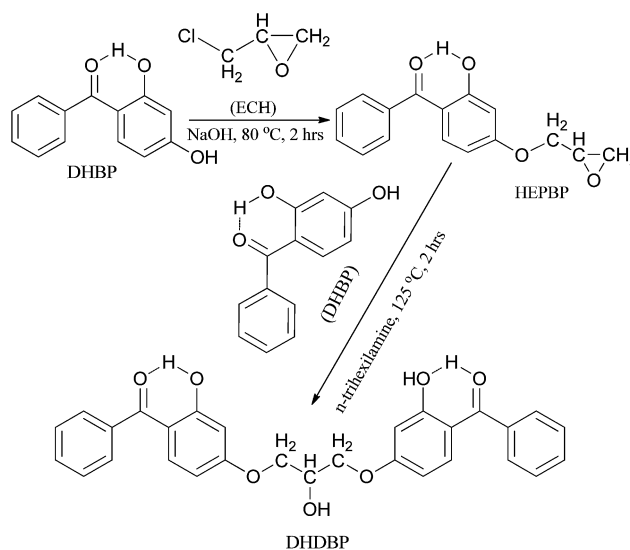


Scheme 1 Synthetic route of 2-hydroxy-4-(3-methacryloxy-2-hydroxypropoxy) benzophenone (BPMA).

Synthesis of DHDBP

The synthetic route of DHDBP is herein shown in Scheme 2.

First, 2-hydroxy-4-(2,3-epoxypropoxy)benzophenone (HEPBP) was synthesized as an intermediate referring to literature.²⁶ Briefly, DHBP (10.72 g, 50 mmol) was dissolved in 50 mL 2 M KOH aqueous solution, afterwards dropped into a 250 mL three-neck flask previously filled with 20 mL ECH at 80 °C under argon protection with mechanical stirring and reflux. Upon the end of dropping, the reaction was maintained 2 h, followed by cooling the liquid to room temperature and washing-separating-washing circularly with deionized water for 6 times. Then the liquid was separated using a separatory funnel and dried over anhydrous magnesium sulfate overnight. After filtrated, the brown liquid was evaporated by a rotary evaporator. The crude product was purified by recrystallization in ethanol



Scheme 2 Synthetic route of 2,2'-dihydroxy-4,4'-(2-hydroxypropoxy) dibenzophenone (DHDBP).

three times, and dried in vacuum till constant weight. DHDBP (2,2'-dihydroxy-4,4'-(2-hydroxypropoxy) dibenzophenone) was synthesized, referring to literature,²⁷ by reaction of DHBP (1.44 g, 6.7 mmol) with HEPBP (2 g, 7.4 mmol) in *o*-xylene (12 mL) under the catalysis of *n*-triethylamine (12 μ L, 0.035 mmol, added with syringe) at 125 °C in a 100 mL three neck round bottom flask with magnetic stirring and reflux under protection of argon, and 2 hours later the liquid was cooled at room temperature overnight to get precipitates. Pure product (with a yield of 46%) was obtained by recrystallization in mixture of ethanol and acetone (5 : 1, v/v) at 78 °C, filtrated and dried in vacuum oven at 40 °C for 48 hours.

Synthesis of HPBP

HPBP (2-hydroxy-4(2,3-dihydroxy propoxy)benzophenone) is the product of the alkaline hydrolysis of HEPBP, and the hydrolytic route can be viewed in Scheme 3.

HPBP was synthesized referring to procedures for preparing similar compounds.²⁸ Briefly, hydrolysis of HEPBP (0.7 g, 2.59 mmol) in 10% NaOH aqueous continued at 60 or 75 °C for 2 h, followed by neutralization with 1 M HCl aqueous till pH = 7. Precipitates produced after cooling the solution in ice-water bath overnight. Pure HPBP was obtained after filtration, washing with deionized water, and drying in vacuum oven at 40 °C for 48 hours. The yield was 48%.

Synthesis of polylactides

Cteyl alcohol, BPMA, DHDBP and HPBP were used respectively as initiators in the ROP of L-lactide to prepare PLA-C, PLA-B, PLA-DB and PLA-HB-PLA, correspondingly, of which PLA-C was prepared as neat PLA for comparison. Each polymerization consumed 2 g L-lactide with varied amount of initiator for desired molecular weights of final PLA products, while the molar ratio of monomer to catalyst, Sn(Oct)₂, is constantly 2000 : 1. The ROP was conducted with magnetic stirring in a glass tube, which was flame dried, evacuated by an oil pump and sealed using an alcohol blow lamp. For PLA-C and PLA-B,

the polymerization temperature was 130 °C, while 145 °C for PLA-DB and PLA-HB-PLA. After 5 hours for each polymerization, the glass tube was rapidly cooled in cold water to room temperature, and then the products were dissolved in chloroform, precipitated in excess ethanol, and finally filtrated after being washed for 3 or more times with ethanol. The precipitate was dried in a vacuum oven at 40 °C to constant weight. The number *e.g.* 100 in PLA-B100, refers to the molar ratio of L-lactide to initiator BPMA. The other polylactides were noted likewise.

Preparation of PLA films

For PLA-C100, PLA-B100, PLA-DB100, PLA-DB400 and PLA-HPBP100-PLA films, they were prepared by solution-casting with the chloroform solutions of the same concentration (5%, w/v). In brief, 0.3 g PLA powder were first dissolved in 6 mL CHCl₃ with magnetic stirring for an hour, followed by casting the solution into a 90 mm diameter Petri dish with flat bottom. The solvent evaporated at room temperature for an hour, and then the films were dried in vacuum overnight. Film samples with average thickness of 40–45 μ m were peeled off the dishes before being subjected to UV-Vis spectrophotometer for transmittance determination.

Nuclear magnetic resonance (NMR)

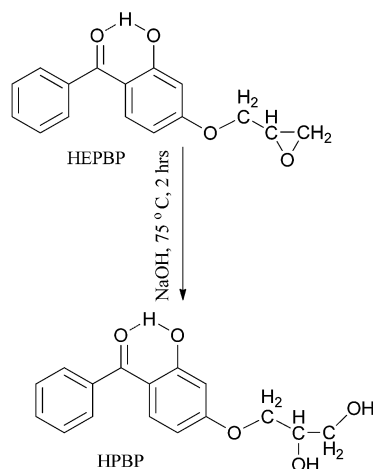
Chemical structures of synthesized UV absorbers (BPMA, DHDBP and HPBP), terminated and blocked PLA were characterized by ¹H NMR spectroscopy with high resolution. The spectra were recorded on a Varian INOVA-400 spectrometer at 400 MHz (or 600 MHz) using deuterated chloroform as solvent and tetramethylsilane (TMS) as internal standard. 5 mg of UV absorbers were dissolved in 0.5 mL CDCl₃ while 6 mg for PLA to enhance the intensity of introduced UV absorption groups on the main chain.

Fourier transform infrared (FTIR) spectroscopy

The FTIR spectra of UV absorbers, terminated and blocked PLA samples were recorded by a Thermo fisher NICOLET IS10 Fourier transform spectrophotometer (USA) in the form of transmission, using KBr as window film. Each sample was scanned 32 times in the range of 4000–400 cm⁻¹, with a resolution of 4 cm⁻¹.

Gel permeation chromatography (GPC)

The molecular weights and their distribution of the polymers were determined in THF on a Shimadzu GPC instrument comprised of a column oven (CTO-20A), a refractive index detector (RID-10A), a degasser (DGPU-20A₃), a pump (LC-20A) and three columns (Shodex KF-803 and KF-804 gel columns, and KF-G guard column). The oven temperature was 40 °C, the flow rate of mobile phase THF was 1.0 mL min⁻¹. Polystyrene standards (10 samples with number average molecular weights in the range of 1300–2 290 000 g mol⁻¹) were used for calibration.



Scheme 3 Synthetic route of 2-hydroxy-4(2,3-dihydroxy propoxy) benzophenone (HPBP).

Differential scanning calorimetry (DSC)

The thermal behavior of PLA-C, PLA-B, PLA-DB and PLA-HB-PLA series products were measured on a NETCS 204 (Germany) DSC instrument. All samples were dried in a vacuum oven at 40 °C for 2 days before DSC measurement. Approximately 5 mg of each PLA sample was sealed in a aluminium pan and scanned at a rate of 10 °C min⁻¹ in the range of 20–190 °C under nitrogen with a flow rate of 50 mL min⁻¹. Then the sample was cooled at the same rate from 190 °C to 30 °C, and heated again from 30 °C to 190 °C. The melting temperature (T_m , peak temperature), cold crystallization temperature (T_{cc}) and degree of crystallization (X_c) were determined. X_c was calculated according to the following equation:

$$X_c = \frac{\Delta H_m - \Delta H_c}{\Delta H_0} \times 100\% \quad (1)$$

where ΔH_m , ΔH_c refers to the enthalpy of fusion and enthalpy of crystallization respectively, during the second heating, and ΔH_0 refers to the enthalpy of fusion of PLA with 100% degree of crystallization, considered as 93 J g⁻¹ according to ref. 29.

Thermogravimetry (TG)

TG measurements were conducted on a NETZSCH TG 209F1 Iris instrument (Germany) under nitrogen atmosphere (with a 60 mL min⁻¹ flow rate) Samples were heated in a Al₂O₃ pan from 25 °C to 500 °C (or 600 °C) at 10 K min⁻¹.

Ultraviolet-visible light (UV-Vis) spectra

The UV-Vis spectra were recorded on a UV-2300 spectrophotometer in the range of 800–190 nm at a scanning rate of 400 nm min⁻¹ at room temperature. The UV absorbers and polylactides were dissolved in 1,4-dioxane for characterization of the absorption spectra, while the solution casting PLA films were subjected directly to the spectrophotometer in transmission mode with air as reference.

Characterization of UV absorbers

The FTIR bands in Fig. 1(A) and NMR chemical shifts in Fig. 1(B) agree well with the previous ref. 25 that has confirmed the chemical structure of BPMA. The strong band at around 1634 cm⁻¹ is assigned to the stretching vibration of ketonic C=O group. The band at 1283 cm⁻¹ is ascribed to the stretching vibration of Ar-C-O, which indicates the successful reaction of the 4-position hydroxyl group. The band at 3525 cm⁻¹ is assigned to the stretching vibration of newly formed alcoholic hydroxyl group. Noticeably, the strong band at 1701 cm⁻¹ is assigned to the stretching vibration of ester carbonyl group C=O. This band shows lower wavenumber due to conjugating with C=C group.

The FTIR and ¹H NMR spectra of DHDBP are plotted separately in Fig. 2(A) and (B). The bands from 3300–3500 cm⁻¹ are assigned to the stretching vibration of hydrogen bonding and non-bonding hydroxyl groups. The weak band at 2876 cm⁻¹ is assigned to the stretching vibration of -CH- group. The band at 1269 cm⁻¹ is assigned to the stretching vibration of Ar-O-C,

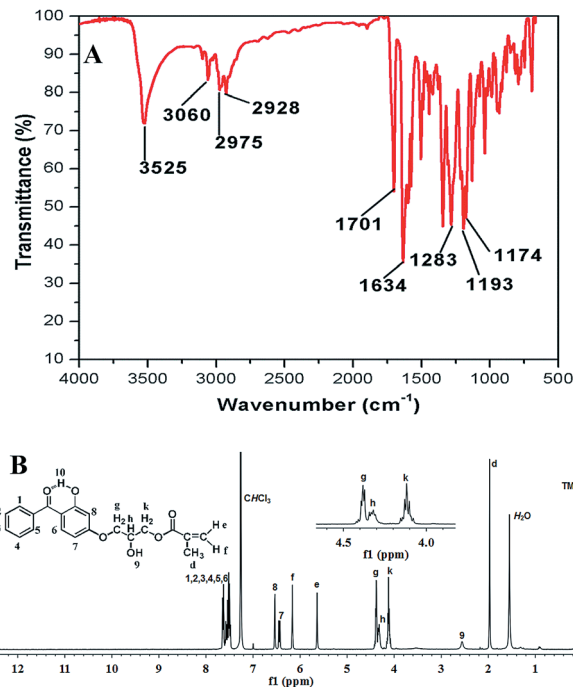


Fig. 1 FTIR transmission spectrum (A) and ¹H NMR spectrum (B) of BPMA.

while that at 1624 cm⁻¹ is assigned to the stretching vibration of ketonic C=O group.

Fig. 3 shows the FTIR transmission and ¹H NMR spectra of HPBP. The broad and strong band at 3375 cm⁻¹ remarkably

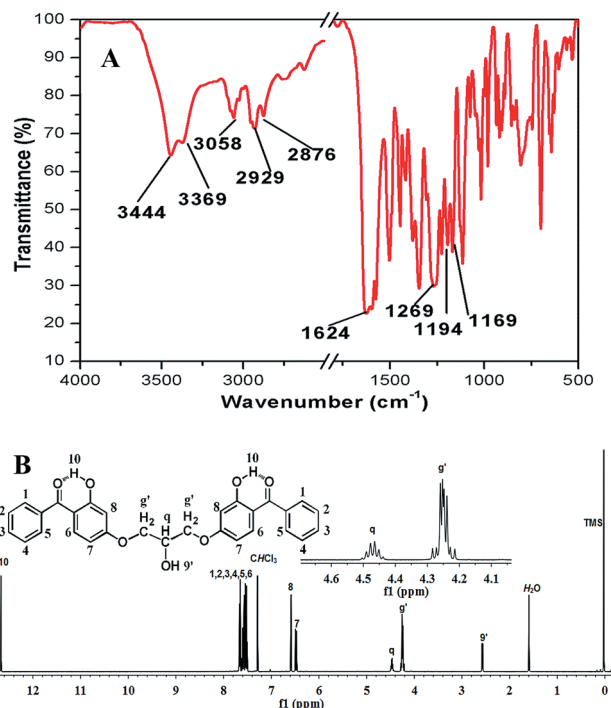


Fig. 2 FTIR transmission spectrum (A) and ¹H NMR spectrum (B) of DHDBP.

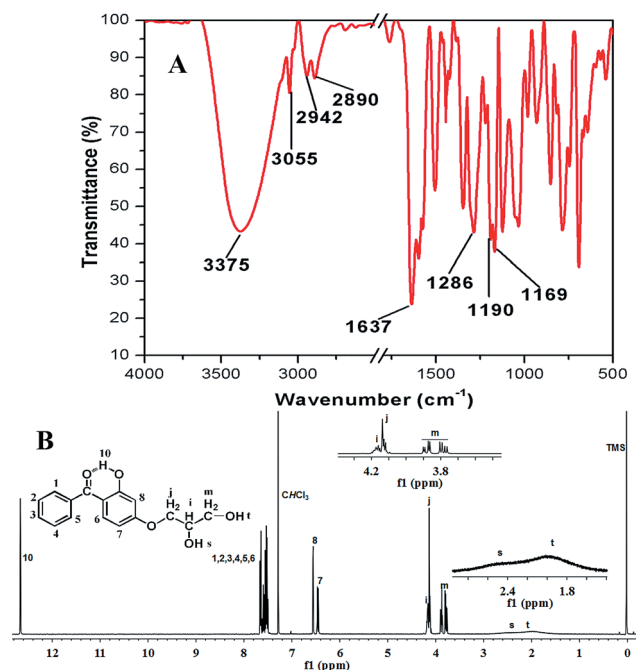


Fig. 3 FTIR transmission spectrum (A) and ^1H NMR spectrum (B) of HPBP.

shown in Fig. 3(A) is assigned to the stretching vibration of newly formed dihydroxyl groups, and there is no sign of band at around 910 cm^{-1} or 1260 cm^{-1} , which are the characteristic bands of epoxy group. This proves the successful hydrolysis of the epoxy group. In the ^1H NMR spectrum of Fig. 3(B), the broad peaks at $\delta = 1.6\text{--}2.7$ are ascribed to H_s and H_t from the two $-\text{OH}$ groups.

The ^1H NMR data are summarized in the following:

BPMA, ^1H NMR (400 MHz, CDCl_3): $\delta = 12.654$ (s, 1H, $-\text{OH}\cdots\text{O}=\text{C}-$), 7.482–7.646 (m, 6H, Ar-H), $\delta = 6.534\text{--}6.540$ (d, $J = 2.4$, 1H, Ar-H), $\delta = 6.427\text{--}6.455$ (dd, $J = 2.4$, 1H, Ar-H), $\delta = 6.165$ (s, 1H, $-(\text{CH}_3)\text{C}=\text{CH}-$, H_f), $\delta = 5.640$ (s, 1H, $-(\text{CH}_3)\text{C}=\text{CH}-$, H_e), $\delta = 4.079\text{--}4.422$ (m, 5H, $-\text{CH}_2\text{-CH-CH}_2-$), $\delta = 2.558$ (s, 1H, $-\text{OH}$), $\delta = 1.974$ (s, 3H, $-\text{CH}_3$).

DHDBP, ^1H NMR (400 MHz, CDCl_3): $\delta = 12.669$ (s, 1H, $-\text{OH}\cdots\text{O}=\text{C}-$), $\delta = 7.647\text{--}7.676$ (m, 4H, Ar-H), 7.577–7.621 (m, 2H, Ar-H), 7.540–7.569 (m, 4H, Ar-H), 7.701–7.525 (m, 2H, Ar-H), 6.583–6.589 (d, $J = 2.4$, 2H, Ar-H), 6.488–6.495 (d, $J = 2.8$, 1H, Ar-H), 6.466–6.472 (d, $J = 2.4$, 1H, Ar-H), 4.438–4.505 (m, 1H, $-\text{CH}_2\text{-CH-CH}_2-$), 4.214–4.284 (m, 4H, $-\text{CH}_2\text{-CH-CH}_2-$), 2.565–2.578 (d, $J = 5.2$, 1H, $-\text{OH}$).

HPBP, ^1H NMR (400 MHz, CDCl_3): $\delta = 12.669$ (s, 1H, $-\text{OH}\cdots\text{O}=\text{C}-$), 7.647–7.676 (m, 2H, Ar-H), 7.579–7.623 (m, 1H, Ar-H), 7.538–7.560 (m, 2H, Ar-H), 7.503–7.527 (m, 2H, Ar-H), 6.560–6.566 (d, $J = 2.4$, 1H, Ar-H), 6.446–6.475 (m, 1H, Ar-H), 4.157–4.205 (m, 1H, $-\text{CH}_2\text{-CH-CH}_2-$), 4.100–4.142 (m, 2H, Ar-O- CH_2-), 3.768–3.905 (m, 2H, $-\text{CH}_2\text{-CH-CH}_2\text{-OH}$), 2.564 (s, 1H, $-\text{CH-OH}$), 2.018 (s, 1H, $-\text{CH}_2\text{-OH}$).

Results and discussion

The synthetic routes and chemical structures of PLA-C, PLA-B, PLA-DB and PLA-HB-PLA are demonstrated in Scheme 4, in which the distributions of UV absorption groups are presented.

Polymer chain structures

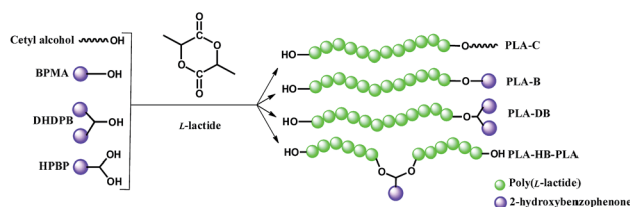
All PLA samples have one of the chain ends terminated by one hydroxyl group except for PLA-HB-PLA, which has each end terminated by one hydroxyl group, and this is confirmed by the integrated area ratio of ending hydroxyl hydrogen (H_s) to that of polymer chain-end methane group (H_b) with a value of 1.

As Fig. 4 shows, for all of the synthesized PLA samples, the peaks at around $\delta = 1.48$ and $\delta = 4.32\text{--}4.40$ are ascribed to H_a and H_b , which belong to $-\text{CH}_3$ and $-\text{CH}-$ respectively near the termination of PLA chain. The peaks at $\delta = 1.57$, 5.14 are ascribed to H_d and H_e that belong to $-\text{CH}_3$ and $-\text{CH}-$ on the main chain of PLA. The peak at $\delta = 2.68$ is ascribed to H_c of the end-capped hydroxyl group of PLA, and this peak is observed in the spectra of all synthesized PLA with different molecular weights but not in the spectrum of PLA-C100 due to high molecular weight. In Fig. 4(A), the triplets at around $\delta = 0.88$ are responsible for H_{11} from end $-\text{CH}_3$ of palmitoyl group, while peaks at $\delta = 1.2\text{--}1.4$ and $\delta = 4.08\text{--}4.20$ are ascribed to H_{12} of $-(\text{CH}_2)_{14}-$ and H_{13} of $-\text{O-CH}_2-$, respectively.²¹

Noticeably, the δ value of H_h ($-\text{CH}-$) in BPMA shifts from 4.28–4.35 to 5.42–5.50 of H_h ($-\text{CH}-$) in PLA-B. This phenomenon of chemical shift was observed likewise in the cases of PLA-DB and PLA-HB-PLA, proving the successful initiated ring opening polymerization of l -lactide by the hydroxyl groups of BPMA, DHDBP and HPBP. For PLA-HB-PLA, especially, the integrated area ratio of ending hydroxyl hydrogen (H_s) to that of polymer chain-end methane group (H_b) is calculated to be 1, indicating that both hydroxyl groups initiated the ROP of l -lactide, thereby proving that the UV absorption group (with 2-hydroxybenzophenone part as pendant) is successfully introduced to the middle of PLA main chain. The other peaks including that on and outside the benzene ring show no chemical shifts in comparison with that of the synthesized UV absorbers. Obviously, the chemical structures of the synthesized poly(lactides) are confirmed by the ^1H NMR spectra presented in Fig. 4.

Molecular weights

The molecular weights of PLA were controlled by adjusting the molar ratio of monomer to initiator, determined by GPC



Scheme 4 Synthetic routes and imagined chain structures of PLA.

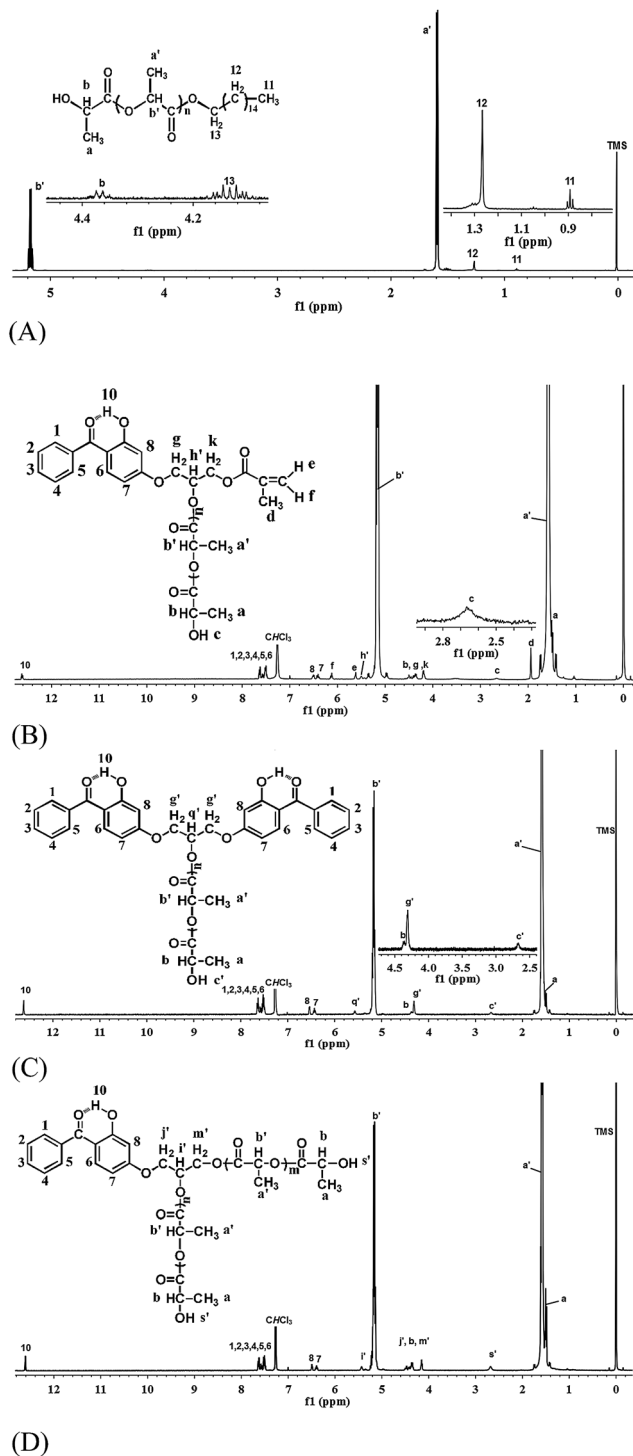


Fig. 4 ^1H NMR spectra of PLA-C (A), PLA-B (B), PLA-DB (C) and PLA-HB-PLA (D).

instrument and also calculated according to ^1H NMR spectra.^{30–33} The calculations are based on integrated area ratio of $\text{O}-\text{CH}(\text{CH}_3)-\text{CO}-$ ($H_{a'}$, 1.57 ppm) and $-\text{CH}_2-(\text{CH}_2)_{14}-\text{CH}_3$ (H_{11} , 0.88 ppm) for PLA-C, $\text{O}=\text{C}-\text{CH}(\text{CH}_3)-\text{O}-$ ($H_{b'}$, 5.14 ppm) and $\text{O}=\text{CH}(\text{CH}_3)-\text{OH}$ (H_b , 4.32–4.40 ppm) for PLA-B and PLA-DB, and $\text{O}=\text{C}-\text{CH}(\text{CH}_3)-\text{O}-$ ($H_{b'}$, 5.14 ppm) and $-\text{OH}\cdots\text{O}=\text{C}-\text{Ar}$

(H_{10} , 12.65 ppm) for PLA-HB-PLA. The GPC traces of polylactides are illustrated in Fig. 5, and related data are summarized in Table 1.

The GPC data listed in Table 1 shows that almost all synthesized samples have very narrow molecular weight distribution except for PLA-DB400 and PLA-C. The latter was obtained by using cetyl alcohol as initiator. For PLA-C, inhomogeneous reaction caused by sudden stop of magnetic stirring and fast solidification of PLA-C product may lead to broad PDI, and higher M_n may be due to impurities or residual water in the reaction that leads to bimodal or even multimodal peaks of GPC curves. On the other hand, the bimodal curves of PLA-DB400 and other PLA-100 are recorded as Fig. 5 presents. This may be due to that the residual water initiates the reaction ahead of the initiator or side reactions like intra- and intertransesterification when $\text{Sn}(\text{Oct})_2$ is used as catalyst.³⁵ The molecular weights determined by GPC can be corrected by multiplying the Mark–Houwink factor of 0.58,³⁴ after which the result is close to theoretical value. The calculated data according to ^1H NMR spectra are close to that of both GPC and the theoretically calculated values, but inaccurate for much higher molecular weights like that of PLA-DB400, which was thereby not subjected to NMR determination. In spite of the existence of measurement errors, the results prove the good quantitative controlling of molecular weights of polylactides using the synthesized UV absorbers as initiators, since the final polymers have close molecular weights on condition of the same ratio of monomer to initiator. Higher molar mass of $65\,476\text{ g mol}^{-1}$ (M_n) suitable for real application is achieved for PLA-DB400 by increasing the monomer–initiator ratio, with the content of UV absorbers in PLA reduced.

Thermal property

The thermal property, mainly crystallization and melting behavior that reflect the polymer chain mobility, were investigated on the synthesized polylactides with different chain structures. The first cooling trace and the second heating trace are plotted in Fig. 6(a) and (b) separately, the cooling and heating DSC traces and TGA curves of PLA-DB400 that has the highest molecular weight are presented in Fig. 7. The thermal data are summarized in Tables 2 and 3.

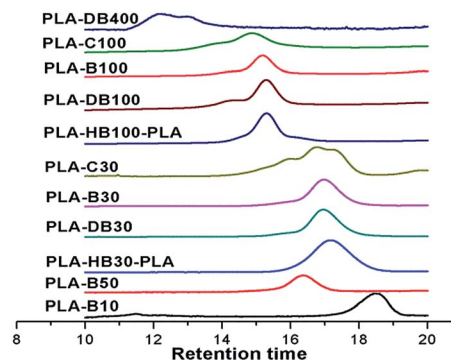


Fig. 5 GPC traces of synthesized polylactides.

Table 1 Yield, molecular weights and PDI of polyactides

Sample	Yield/%	M_n ,NMR ^a	M_n ,GPC ^b	M_n ,CAL ^c	PDI ^d
PLA-DB400	96	— ^e	65 476	55 833	1.60
PLA-C100	90	15 984	16 119	13 215	1.20
PLA-B100	89	13 338	13 428	13 185	1.07
PLA-DB100	89	13 808	13 182	13 356	1.10
PLA-HB100-PLA	83	12 131	11 707	12 000	1.06
PLA-C30	90	4004	5733	4134	1.16
PLA-B30	95	4234	5054	4464	1.08
PLA-DB30	83	4232	5070	4086	1.06
PLA-HB30-PLA	77	3632	4391	3608	1.09
PLA-B50	89	5070	7117	6747	1.06
PLA-B10	81	1769	2143	1531	1.08

^a Calculated according to $^1\text{H NMR}$, $M_n = (A(H_x)/A(H_y)) \times 72.069 + M_i$ ($x = a'$, $y = 11$ for PLA-C; $x = b'$, $y = b$ for PLA-B and PLA-DB; $x = b'$, $y = 10$ for PLA-HB-PLA; A refers to integrated area, M_i is the molar mass of the initiator, and 72.069 is half of the molecular weight of the monomer).
^b GPC results corrected by multiplying 0.58.³⁴ ^c Theoretically calculated, $M_n = 144.137$ (molecular weight of monomer) $\times [\text{LA}]_0/[\text{I}]_0 \times \text{yield} + M_i$.
^d Polydispersity index. ^e — refers to not determined.

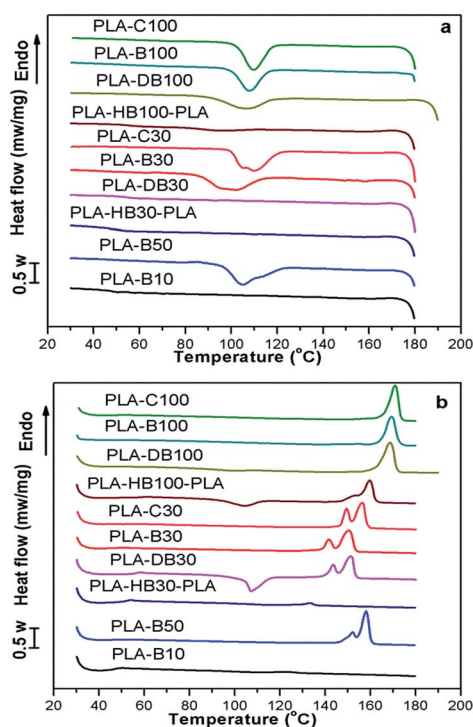


Fig. 6 DSC cooling (a) and second heating (b) curves under non-isothermal condition (10 K min^{-1}).

Table 2 shows that among the PLA-100 samples, PLA-B100 and PLA-DB100 have similar T_{cc} , T_m values and close X_c to that of PLA-C100, indicating that the restriction of large end-capping groups from BPMA and DHDBP on polymer chain mobility are too weak to influence the crystallization. And for PLA-DB400, its X_c value is comparable to that of PLA-B100 and PLA-DB100, while its T_{cc} is several centigrade lower and T_m a little higher due to higher molecular weight. But the blocked

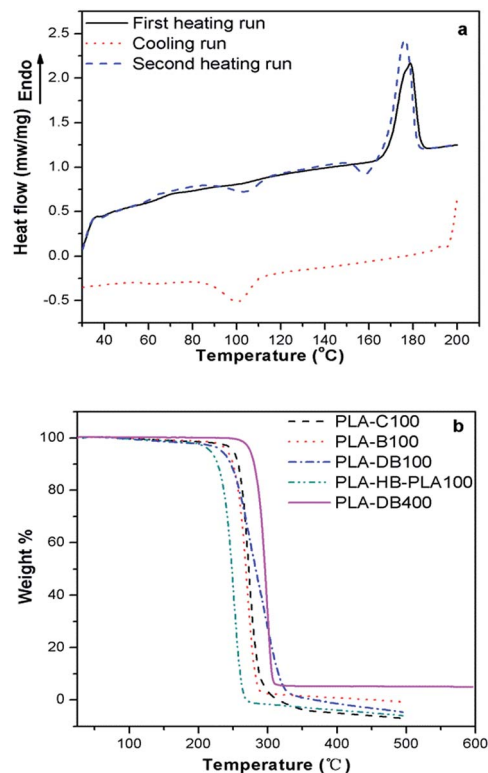


Fig. 7 DSC curves (a) of PLA-DB400 and TG curves (b) of PLA-DB400 and PLA-100.

PLA-HB100-PLA with similar M_n shows a $10 \text{ }^\circ\text{C}$ decrease in T_{cc} and T_m , and a significant decrease in X_c which is only 25.1% compared to 58.4–71% of the previous three ones. This proves that PLA-HB100-PLA can still crystallize though the crystallization is delayed due to the steric hindrance of the blocked HPBP unit. With decrease in M_n to be around 4000, the T_{cc} of PLA-C30, PLA-B30 and PLA-DB30 are close and similar to that of the PLA-100 but the T_m values are about $20 \text{ }^\circ\text{C}$ lower. T_m is herein affected by the molecular weight obviously, and the double melting behavior as other researchers mentioned are observed here as well, including that of PLA-B50 with M_n of about 6000. It is explained by Yasuniwa³⁶ to be melt-recrystallization mechanism and confirmed by the research of Y. He *et al.*³⁷ As explained, the peak at lower temperature is assigned to the primary crystallizes formed during cooling process, while the peak at higher temperature is relatively perfect lamella stacks formed during the second heating. Moreover, both PLA-C30 and PLA-B30 show an X_c value of about 60%, close to that of PLA-100, but PLA-DB30 and PLA-HB30-PLA seem not to crystallize under the same cooling condition as their X_c are lower than 8%, and the crystallization peaks could hardly be observed in Fig. 6(a). Apparently, the above results support that when the M_n are as low as about 4000, the large volume and rigidity of end-group from DHDBP drastically weaken the crystallization ability, and the UV absorption group as pedant group from the blocked unit of HPBP greatly restrict the polymer chain mobility, resulting in extremely low degree of crystallization of PLA-DB30 and PLA-HB30-PLA. As for PLA-B10, it has the lowest

Table 2 Thermal parameters of synthesized polylactides obtained by DSC measurement

Sample	T_{cc}^a (°C)	T_{m1}^b (°C)	T_{m2}^b (°C)	ΔH_{cc}^c (J g ⁻¹)	ΔH_c^d (J g ⁻¹)	ΔH_m^d (J g ⁻¹)	X_c^d (%)
PLA-C100	109.7	—	171.0	-50.15	0	66.04	71.0
PLA-B100	108.0	—	169.4	-42.55	0	54.3	58.4
PLA-DB100	106.3	—	168.7	-40.01	-4.943	62.55	61.9
PLA-DB400	99.9	—	176.2	-22.22	-5.772; -8.833	68.47	57.9
PLA-HB100-PLA	95.6	—	159.7	-6.942	-27.53	50.86	25.1
PLA-C30	110	149.4	156.4	-54.78	0	57.13	61.4
PLA-B30	102.1	141.7	150.4	-51.35	0	58.53	63
PLA-DB30	107.3	143.5	151.3	0	-47.33	53.89	7.1
PLA-HB30-PLA	—	—	133.4	0	0	5.263	5.7
PLA-B50	104.8	152.1	158.1	-57.27	0	61.35	66
PLA-B10	—	—	—	0	0	0	0

^a T_{cc} is cold crystallization temperature. ^b T_{m1} and T_{m2} are peak temperatures of melting. ^c ΔH_{cc} is cold crystallization enthalpy. ^d ΔH_c and ΔH_m are crystallization enthalpy and melting enthalpy, respectively, during second heating; X_c is degree of crystallization.

Table 3 Thermal stability parameters of PLA from TGA test

Sample	$T_{d-5\%}^a$	$T_{d-10\%}^b$	T_{d-max}^c
PLA-DB400	274.8	280.4	299.1
PLA-C100	250.2	257.7	272.8
PLA-B100	242.7	250.2	270.2
PLA-DB100	235.2	247.7	272.7
PLA-HB-PLA100	217.7	227.7	250.8

^a $T_{d-5\%}$ is onset decomposition temperature (at 5% weight loss). ^b $T_{d-10\%}$ refers to the temperature with 10 wt% decomposed. ^c T_{d-max} refers to the temperature at the highest rate of decomposition.

molecular weight and could not crystallize at the cooling rate of 10 K min⁻¹. This is due to that PLA-B10 has much too low molecular weight and short polymer chain but higher content end-capping UV groups which more seriously hinder the segmental mobility.¹⁹ Apparently, macromolecular structure has significant influence on the crystallization behaviors of PLA, especially for PLA-HB-PLA as a triblock copolymer. Although the DP value of PLA-HB-PLA is as low as 1, the influence of introduced UV absorption group as pedant on the crystallization is drastic and should not be ignored. And, the effect of end-capping group with large volume and rigidity on crystallization is remarkable as well when the M_n is around 4000, but greatly weakened when M_n is much higher.

As Fig. 7(b) and Table 3 show, the thermal stability of synthesized PLAs are dependant on the molecular weight, since the thermal parameters including $T_{d-5\%}$, $T_{d-10\%}$ and T_{d-max} show a trend of decreasing with the decreasing of PLA molecular weights. PLA-DB400 possess the highest onset decomposition temperature at 274.8 °C and temperature of fastest rate of decomposition at 299.1 °C because of its high molecular weight ($M_n > 65\ 000$). These data promise PLA-DB400 applicable.

Effect of UV absorber content and position on UV-Vis opacity

As the UV absorbers are used as initiators, molecular weights of the synthesized PLAs are controlled by monomer-initiator ratios, indicating that different molecular weights present different contents of UV absorbers. Fig. 8 shows UV absorption

properties of all synthesized UV absorbers and polylactides in 1,4-dioxane.

It can be seen that the light with wavelength longer than 380 nm are not absorbed. The maximum absorption peaks at 325 nm result from the n- π^* transition of carbonyl group of 2-hydroxybenzophenone part, while that at 285 nm result from the π - π^* transition of phenyl group. The absorbance of HPBP is a little higher than that of BPMA at the same molar concentration, but that of DHDBP is comparable at only half concentration of the previous ones, proving that DHDBP has the strongest UV absorption property among the three.

The wavelength at maximum absorbance (λ_{max}) for PLA-B100, PLA-DB100, and PLA-HB100-PLA are the same with that of BPMA, DHDBP and HPBP, respectively, as shown in Fig. 8, and no wavelength shift is observed. At the same concentration, PLA-B100 and PLA-HB100-PLA show similar absorbance while PLA-DB100 has much stronger absorbance, which agrees with the fact that PLA-DB bears two 2-hydroxybenzophenone groups, hence improving the absorption effect of PLA-DB. Thereby, the

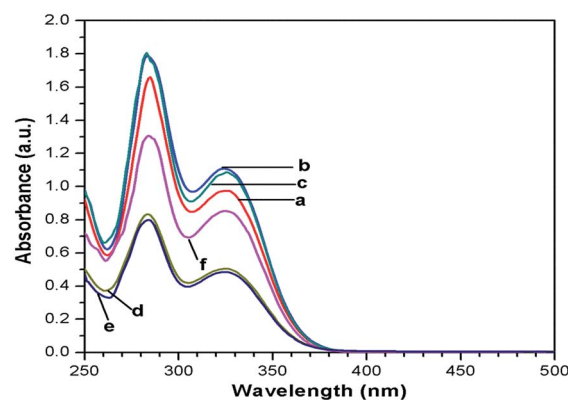


Fig. 8 UV absorption spectra of BPMA ((a), 1×10^{-4} mol L⁻¹), HPBP ((b), 1×10^{-4} mol L⁻¹), DHDBP ((c), 5×10^{-5} mol L⁻¹, as DHDBP containing two DHBP groups), PLA-B100 ((d), 0.74 g L⁻¹), PLA-HB100-PLA ((e), 0.74 g L⁻¹) and PLA-DB100 ((f), 0.74 g L⁻¹) in 1,4-dioxane (the concentration of all polylactides here corresponds to a concentration of 5×10^{-5} mol L⁻¹ of DHBP group, half that of the UV absorber monomers).

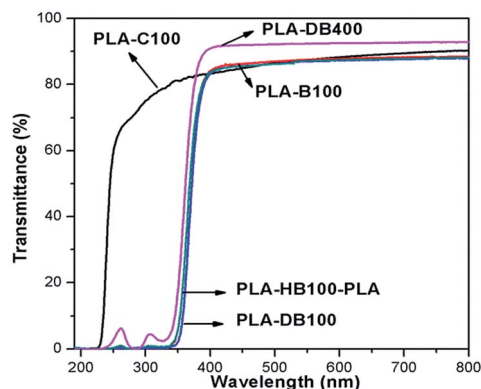


Fig. 9 UV-Vis transmittance spectra of PLA-C100, PLA-B100, PLA-DB100, PLA-DB400 and PLA-HB100-PLA films.

above results indicate that the position of introduced UV absorption groups on the polymer chain has no effect on the UV absorption property of final polylactides while the content plays a crucial role in the absorbance.

Fig. 9 shows the UV-Vis transmittance of the polylactide films (with thickness in the range of 40–45 μm). It is apparent that PLA-C100 film has high transmittance in the region of 220–800 nm, while the other films containing UV absorbers show almost no transmission of UV light under 350 nm, and have transparency higher than 85% above 400 nm, regardless of the content and position of the introduced UV absorption groups. Especially, PLA-DB400 with the least content of UV absorbers and the highest molecular weight show the best transparency and little transmission of UV light under 350 nm. This clearly shows that in the case of films with thickness of 40–45 μm , the prepared films with UV absorption groups covalently bonded have good transparency in visible light region and good UV blocking ability even with only one UV absorption group on the main chain. But increase in content of the UV absorption group, as PLA-DB100 and PLA-DB400 shows, has little effect on expanding the absorption to the whole UV light region. Herein in terms of PLA-DB that has higher content of UV absorber, it is allowed to use less amount of DB as initiator to prepare PLA-DB400 with higher molecular weight ($M_n \approx 65\,000\text{ g mol}^{-1}$) and similar good UV blocking effect. The above results suggest that the introduction of UV absorption groups into PLA chain can effectively block the transmission of most UV light that are not absorbed by neat PLA products, and can keep the high transparency of PLA regardless of the position of the UV absorption groups, making it a potential packaging materials with combination of biodegradability and UV resistance.

Conclusions

Three different UV absorbers were synthesized and used as initiators in the ROP of L-LA successfully, and the chemical structures of the UV absorbers, terminated and blocked polylactides were confirmed. Molecular weights determination and calculation proved a good control of molecular weights of final polylactides. DSC results reveal that both molecular weight and

chain structure have significant influence on the crystallization properties of the polymer. When the molecular weights are around 12 000, the blocked HPBP unit drastically delay and restrict the crystallization of PLA, while the end-capping group from cetyl alcohol, BPMA and DHDBP show similar effect that is too weak to influence the crystallization. With lower molecular weights of around 4000, both end-capping of DHDBP and blocking of HPBP show great steric hindrance of chain mobility resulting in drastic decrease in crystallization ability. Further decrease in M_n like that of PLA-B10 leads to shorter polymer chain and stronger hindering effect of end groups, thus no crystallization is observed. TGA results reveal that with increase of molar mass to be above 65 000, PLA-DB400 show the best thermal stability. Besides, as DHPBP bears two UV absorption groups, it allows for achieving higher molar mass for applications including packaging and maintaining good UV blocking effect of PLA simultaneously. Finally, improvement of the concentration of UV absorption group shows great enhancement in the UV absorbance while the position of introduced UV absorption groups has no influence on the UV absorption property or transparency.

Acknowledgements

The authors appreciate financial supports from National Natural Science Foundation of China (no. 50873067 and 51133005) and Research Fund for the Doctoral Program of Higher Education of China (no. 20110181110032).

References

- 1 S. Slomkowski, S. Penczek and A. Duda, *Polym. Adv. Technol.*, 2014, **25**, 436–447.
- 2 E. S. Place, J. H. George, C. K. Williams and M. M. Stevens, *Chem. Soc. Rev.*, 2009, **38**, 1139.
- 3 P. R. G. Ray, E. Drumright and D. E. Henton, *Adv. Mater.*, 2000, **12**, 1841–1846.
- 4 K. Madhavan Nampoothiri, N. R. Nair and R. P. John, *Bioresour. Technol.*, 2010, **101**, 8493–8501.
- 5 S. Jacobsen and H. G. Fritz, *Polym. Eng. Sci.*, 1999, **39**, 1303–1310.
- 6 N. Burgos, D. Tolaguera, S. Fiori and A. Jiménez, *J. Polym. Environ.*, 2013, **22**, 227.
- 7 Y. Byun, Y. T. Kim and S. Whiteside, *J. Food Eng.*, 2010, **100**, 239–244.
- 8 M. Murariu, A. Da Silva Ferreira, M. Alexandre and P. Dubois, *Polym. Adv. Technol.*, 2008, **19**, 636–646.
- 9 R. Auras, B. Harte and S. Selke, *Macromol. Biosci.*, 2004, **4**, 835–864.
- 10 C. Zhang, C. Man, W. Wang, L. Jiang and Y. Dan, *Polym.-Plast. Technol. Eng.*, 2011, **50**, 810–817.
- 11 A. V. Janorkar, A. T. Metters and D. E. Hirt, *J. Appl. Polym. Sci.*, 2007, **106**, 1042–1047.
- 12 C. Man, C. Zhang, Y. Liu, W. Wang, W. Ren, L. Jiang, F. Reisdorffer, T. P. Nguyen and Y. Dan, *Polym. Degrad. Stab.*, 2012, **97**, 856–862.

- 13 M. Murariu, A. Doumbia, L. Bonnaud, A. L. Dechief, Y. Paint, M. Ferreira, C. Campagne, E. Devaux and P. Dubois, *Biomacromolecules*, 2011, **12**, 1762–1771.
- 14 M. Mucha, S. Bialas and H. Kaczmarek, *J. Appl. Polym. Sci.*, 2014, **131**, 40144.
- 15 D. D. Ye, C. Y. Xiao, R. R. Qi and P. K. Jiang, *J. Appl. Polym. Sci.*, 2012, **125**, E117–E124.
- 16 S. Therias, J. F. Larche, P. O. Bussiere, J. L. Gardette, M. Murariu and P. Dubois, *Biomacromolecules*, 2012, **13**, 3283–3291.
- 17 S. R. Andersson, M. Hakkarainen and A.-C. Albertsson, *Polym. Degrad. Stab.*, 2012, **97**, 914–920.
- 18 V. P. J. Luston and F. Vass, *J. Appl. Polym. Sci.*, 1993, **48**, 219–224.
- 19 I. M. Martinez de Arenaza, J. R. Sarasua, H. Amestoy, N. Lopez-Rodriguez, E. Zuza, E. Meaurio, F. Meyer, J. I. Santos, J. M. Raquez and P. Dubois, *J. Appl. Polym. Sci.*, 2013, **130**, 4327–4337.
- 20 I. Rashkov, N. Manolova, S. M. Li, J. L. Espartero and M. Vert, *Macromolecules*, 1996, **29**, 50–56.
- 21 D. Koo, A. Du, G. R. Palmese and R. A. Cairncross, *Polym. Chem.*, 2012, **3**, 718.
- 22 J. Zhou, Z. Jiang, Z. Wang, J. Zhang, J. Li, Y. Li, J. Zhang, P. Chen and Q. Gu, *RSC Adv.*, 2013, **3**, 18464.
- 23 C.-P. Wu, C.-C. Wang and C.-Y. Chen, *J. Polym. Sci., Part B: Polym. Phys.*, 2014, **52**, 823–832.
- 24 R. Auras, L.-T. Lim, S. E. M. Selke and H. Tsuji, *Poly(lactic acid) – Synthesis, Structures, Properties, Processing and Applications*, Wiley, New Jersey, 2010, ch. 22, p. 388.
- 25 Y. Zhao and Y. Dan, *Eur. Polym. J.*, 2007, **43**, 4541–4551.
- 26 S. Olsson, M. Johansson, M. Westin and E. Ostmark, *Polym. Degrad. Stab.*, 2012, **97**, 1779–1786.
- 27 A. T. Shigeo TANIMOTO, *Bull. Inst. Chem. Res., Kyoto Univ.*, 1991, **69**, 560–570.
- 28 Y. Liu, L. Zou, L. Ma, W. H. Chen, B. Wang and Z. L. Xu, *Bioorg. Med. Chem.*, 2006, **14**, 5683–5690.
- 29 E. W. Fisher, H. J. Sterzel and G. Wegner, *Kolloid Z. Z. Polym.*, 1973, **251**, 980–990.
- 30 T. C. Ward, *J. Chem. Educ.*, 1981, **58**, 867–879.
- 31 E. M. Todd and S. C. Zimmerman, *J. Am. Chem. Soc.*, 2007, **129**, 14534–14535.
- 32 G. W. Nyce, T. Glauser, E. F. Connor, A. Mock, R. M. Waymouth and J. L. Hedrick, *J. Am. Chem. Soc.*, 2003, **125**, 3046–3056.
- 33 J. U. Izunobi and C. L. Higginbotham, *J. Chem. Educ.*, 2011, **88**, 1098–1104.
- 34 A. D. Jolanta Baran, A. Kowalski, R. Szymanski and S. Penczek, *Macromol. Rapid Commun.*, 1997, **18**, 325–333.
- 35 W. W. Wang, W. Y. Ren, L. Jiang and Y. Dan, *J. Appl. Polym. Sci.*, 2010, **118**, 2379–2388.
- 36 M. Yasuniwa, S. Tsubakihara, Y. Sugimoto and C. Nakafuku, *J. Polym. Sci., Part B: Polym. Phys.*, 2004, **42**, 25–32.
- 37 Y. He, Z. Fan, Y. Hu, T. Wu, J. Wei and S. Li, *Eur. Polym. J.*, 2007, **43**, 4431–4439.